PCCP

Oxygen adsorption onto pure and doped Al surfaces – the role of surface dopants

Journal:	*Physical Chemistry Chemical Physics*
Manuscript ID:	CP-ART-09-2014-004277.R1
Article Type:	Paper
Date Submitted by the Author:	28-Oct-2014

Complete List of Authors:	Lousada Patricio, Claudio; KTH Royal Institute of Technology, Materials Science and Engineering Korzhavyi, Pavel; KTH Royal Institute of Technology, Materials Science and Engineering

Oxygen adsorption onto pure and doped Al surfaces – the role of surface dopants

Cláudio M. Lousada* and Pavel A. Korzhavyi

Division of Materials Technology, Department of Materials Science and Engineering,
KTH Royal Institute of Technology, SE-100 44 Stockholm, Sweden

* To whom correspondence should be addressed: phone, (46) 879 06 252; e-mail, cmlp@kth.se

TOC Image

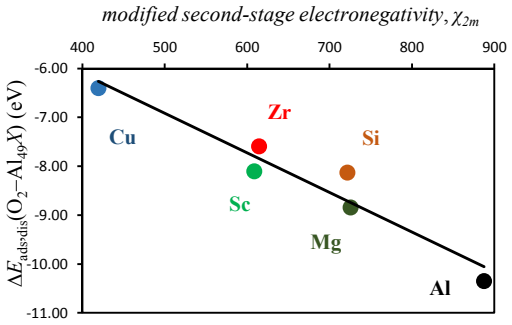

TOC Image. Dissociative adsorption energy of O_2 at a doped (111) surface of an Al_{49} cluster: $\Delta E_{ads,dis}(O_2–Al_{49}X)$ (eV) as a function of the Mulliken *modified second-stage electronegativity* of the dopant atom, χ_{2m}.

Abstract

Using density functional theory (DFT) with the PBE0 density functional we investigated the role of surface dopants on the molecular and dissociative adsorption of O_2 onto Al clusters of the type: Al_{50}, $Al_{50}Al_{ad}$, $Al_{50}X$ and $Al_{49}X$ where X represents a dopant atom of the following elements: Si, Mg, Cu, Sc, Zr, Ti. Each dopant atom was placed at the Al(111) surface as an adatom or as a substitutional atom, in the last case replacing a surface Al atom. We found that for the same dopant geometry, the closer is the ionization energy of the dopant element to that of elemental Al, the more exothermic is the dissociative adsorption of O_2 and the stronger are the bonds between the resulting O atoms and the surface. Additionally we show that the Mulliken concept of electronegativity can be applied in the prediction of the dissociative adsorption energy of O_2 onto the doped surfaces. The Mulliken *modified second-stage electronegativity* of the dopant atom is proportional to the exothermicity of the dissociative adsorption of O_2. For the same dopant element in an adatom position the dissociation of O_2 is more exothermic when compared to the case where the dopant occupies a substitutional position. These observations are discussed in view of the overlap population densities of states (OPDOS) computed as the overlap between the electronic states of the adsorbate O atoms and the clusters. It is shown that a more covalent character in the bonding between the Al surface and the dopant atom causes a more exothermic dissociation of O_2 and stronger bonding with the O atoms when compared to a more ionic character in the bonding between the dopant and the Al surface. The extent of the adsorption site reconstruction is dopant atom dependent and an important parameter for determining the mode of adsorption, adsorption energy and electronic structure of the product of O_2 adsorption. The PBE0 functional could predict the existence of the O_2 molecular adsorption product for many of the cases here investigated.

Introduction

Interactions between oxygen and aluminum are of interest for many technological applications that involve this metal, such as catalysis and diverse areas of materials technology.[1] Aluminum, the most abundant metal in the earth's crust, is already used in a wide variety of processes but still finds innovative usages in many different applications. Upon exposure to oxygen, aluminum metal surfaces are readily passivated by a layer of oxide which enhances their corrosion resistance.[2] The high exothermicity of the reaction of aluminum with oxygen leads to the formation of an oxide which is thermodynamically stable under a wide variety of conditions.[3] Understanding the interactions between oxygen and aluminum is thus important in order to further improve and better predict the performance of aluminum based materials.

Gaining detailed knowledge of the interactions, adsorption and further reactions of O_2 with metal surfaces is challenging for both experimental and theoretical approaches.[4] This is mostly due to the fact that these processes are fast and involve changes in the spin state of O_2 as the gas-phase molecule interacts with surfaces of metals.[5] It is known with basis on experimental[1, 6, 7] and theoretical[1, 7-9] investigations that the reaction of dissociation of O_2 at Al surfaces is very fast: the molecular adsorption product of O_2 has little stability and consequently it is short-lived. Nevertheless, at the Al(111) surface, the molecular adsorption of O_2 occurs leading to a stable product.[8, 9] The adsorption of the O atoms resultant from the dissociation of O_2 is generally considered as the initial step of the process of oxidation of Al.[8, 10-12] The fact that an energy barrier for O_2 adsorption is not predictable in many computational studies has been attributed to the limitations of single determinant electronic structure calculation methods in describing the triplet-singlet transition that occurs in O_2 when the molecule starts to interact with a metal surface.[4, 13] The change in spin multiplicity in O_2—that is subject to the Wigner spin selection rules—has been appointed as one of the main underlying causes for the existence of an energy barrier for the homolytic cleavage of the O-O bond in O_2 at metal surfaces.[5, 14] Other phenomena

such as non- local exchange effects[15] or short-ranged correlation effects[13] have also a contribution for the existence of the energy barrier for O_2 cleavage. All these phenomena are at the origin of the low dissociative sticking probability[7, 16] (<0.01) for O_2 at Al(111).[17] Additionally, the presence of other chemical elements at the surface of Al is known to affect the chemistry and dynamics of the interactions of O_2 with these surfaces.[18] These systems present an additional level of complexity in what concerns the electronic structure of the surface-adsorbate complex when compared with a surface of a pure metal.

It has been shown experimentally that the adsorption of O_2 on Al(111) at low temperatures between [85-150] K gives rise to close-spaced dimers of surface bound O atoms which are distributed at the surface at large separations—of several tenths of Å between dimers.[19] The spacing between the O atoms in the dimers lays in the range of one to three Al interatomic distances. In the cited study it was found that even though these O atoms are close-spaced, they are not bound to each other and are in the form of atomic O. The underlying reason for the close spacing of these species might reside on the fact that after homolytic O_2 splitting, due to their strong interactions with the surface, the adsorption of the resulting O atoms is very exothermic—in the order of 5 eV per O atom.[11] This fact, together with the interactions between the O atoms, limits the surface mobility of the O atoms at low temperatures. A reason for the apparent randomness of the surface distribution of O dimers has not been appointed but based on the existing knowledge of the effect of surface defects in lowering many energy barriers for homolytic bond cleavage in adsorbates, the role of surface defects should not be excluded as an underlying cause for this apparent randomness.[20]

The adsorption of O_2 onto a metal surface is accompanied by charge transfer from the surface to the O_2 molecule. The lowest unoccupied molecular orbital (LUMO) of O_2 is an anti-bonding $2\pi^*$ orbital. Populating this orbital leads to the weakening and ultimately to the splitting of the

bond in O_2. In spite of the challenges which electronic structure methods face for correctly describing the chemistry of O_2 at metal surfaces,[21] hybrid DFT functionals could previously successfully grasp the details of the molecular adsorption structure and the energy barrier for splitting the O_2 molecule at the Al(111) surface.[22] The pure DFT functionals based only on the generalized gradient approach (GGA) or local density approximation (LDA) fail to account for an energy barrier for dissociative adsorption of O_2 and thus cannot locate the molecular adsorption structure in the adiabatic potential energy surface.[5, 8, 23, 24] The reason for this discrepancy with experiments has been attributed to the fact that the energy of the LUMO of O_2 as predicted by GGA or LDA type of functionals lays below the Fermi level of Al.[22] According to the authors, this makes the charge transfer from the Al surface to O_2 a spontaneous and barrierless process when described with such functionals. The hybrid DFT functionals place the LUMO orbital of O_2 at energies above the Fermi level of Al and consequently can account for the existent of an energetic barrier for electron transfer from the surface to the O_2 orbitals. This suggestion that hybrid DFT is always able to predict the existence of a barrier for the cleavage of O_2 in view of the placement of the electronic energy levels of O_2 and of the surface will be discussed in this work.

In this work, we report the results of the investigation of the effect of the presence of dopant atoms on the adsorption of O_2 onto the Al(111) surface using DFT. This study compares the adsorption of O_2 onto a plane Al(111) surface and onto surfaces where one dopant atom of the following elements was added: Zr, Ti, Si, Sc, Mg, and Cu. Two types of geometry for the dopant atom were investigated: one consisting of the dopant as an adatom; the second is the case where the dopant substitutes a Al(111) surface atom—making a plane Al(111) surface with a substitutional impurity. We found that both the type of doping element and its disposition at the

Al(111) surface can greatly affect the bonding, the mechanism and the energetics of O_2 adsorption at the Al(111) surface.

Computational Details

The DFT calculations were performed using cluster[25] models of Al and the software package Jaguar 7.9 (Ref. 26). The geometry optimizations were done with the hybrid density functional PBE0 (Ref. 27,28). The PBE0 functional has previously provided a good description of the electronic properties and structures of Al clusters.[29, 30] For geometry optimizations, the all electron 6-31G basis set was employed for non-transition metal atoms. This implies 13 basis functions per Al atom. For the transition-metal atoms: Zr, Cu, Ti, Sc, the LACVP basis set was used. The basis set LACVP is a combination of the split valence basis set 6-31+G(d) and the Los Alamos effective core potential (ECP) (Ref. 31) for transition metals. The single point energy calculations were done using the split valence, all electron triple-ζ basis set 6-311G++** for non-transition metals, which corresponds to 21 basis functions per Al atom. This basis set supplements all atoms with polarization and diffuse functions. The transition metals were treated with the LACV3P++** basis set which is the triple-ζ implementation of the LACVP basis set and augments the transition metal basis set with polarization and diffuse functions. The effect of the addition of an *a posteriori* term of the D3 type to the energies obtained with PBE0, for accounting for dispersion interactions was also investigated. This is the zero-damping, two-body only correction as previously suggested by Grimme *et al*.[32, 33] Tight convergence criteria and ultrafine integration grids were used for all the calculations (atomic units): rms gradient $< 3 \times 10^{-4}$; maximum gradient $< 4.5 \times 10^{-4}$; rms step $< 1.2 \times 10^{-3}$; maximum step $< 1.8 \times 10^{-3}$; maximum change in total energy between two consecutive steps $< 5 \times 10^{-5}$.

The adsorption energies reported herein were calculated as

$$\Delta E_{ads} = E_{adsorbate/cluster} - (E_{adsorbate} + E_{cluster})$$

where $E_{adsorbate/cluster}$, $E_{adsorbate}$, $E_{cluster}$, represent the 0 K electronic energies in gas-phase for the adsorbate binding to the cluster, free adsorbate and bare cluster respectively. This definition means that the more negative is the adsorption energy, the stronger is the adsorption. The cluster models implemented here conform to the three principles proposed to model metal oxides using clusters.[34, 35] These principles are the neutrality principle, the stoichiometry principle and the coordination principle.

The electronic structure descriptors such as density of states and orbital analysis were done using the software package AOMix.[36] The methods used to compute the overlap population density of states (OPDOS) as well as the contribution of O atoms orbitals to bonding, both as a function of the orbital energies are the standard methods employed[37, 38] and described in AOMix. The fragments considered for computing the OPDOS consist of the clusters (fragment 1) and the O atoms (fragment 2). The OPDOS shown and discussed in this work are the result of the overlap between the electronic states of these two fragments. The OPDOS computation method allows the determination of the contribution of the orbitals of a given fragment—at certain energies—to the one-electron levels of a product where such fragment is part of. OPDOS plots use Mulliken population analysis[39] (MPA) as a method for the electron population analysis. When used to study changes on electron populations due to adsorption[40] or to compare the electron populations of clusters that only differ slightly in chemical composition,[41] the MPA approach has proved to be a reliable method.

Results and discussion

Pure Al clusters

It has been demonstrated previously that adsorption and further reactions on surfaces of pure metals and alloys can be fairly well modelled using cluster models provided that low coverages of adsorbates are considered.[18, 42-44] The clusters of Al used in this work were built following

some fundamental criteria recurrently suggested to model surfaces using cluster models.[45] The clusters were built keeping in mind that these properties should be conserved when the surfaces are sliced from the extended crystal structures. It has been shown additionally that a high level of symmetry is a desirable feature of cluster models of metals in order to avoid instabilities in the corresponding wave-function and to speed up its determination.[46] The clusters used in this work are of the type Al_{50} (C_{3v}), $Al_{50}Al_{ad}$, $Al_{50}X_{ad}$ and $Al_{49}X_{sub}$, —with X representing surface dopant: *ad* in adatom position and *sub* in substitutional position replacing a Al(111) atom. The dopants considered are: Si, Mg, Cu, Sc, Zr and Ti. These clusters have the highest symmetry possible for a 50 atom pyramidal-shaped cluster based on the (111) surface cut from an fcc crystal structure. For the geometry optimizations, the coordinates of the (111) surface and of the inner atoms were allowed to relax while the coordinates of the atoms composing the other facets of the clusters were kept fixed.

It has been also previously illustrated the need for using an all electron basis set for accurately describing the chemistry of higher oxidation states of Al.[47] For the present work, this fact was taken into account given that the goal is to investigate the molecular adsorption of O_2, its cleavage and the formation of the first Al-O bonds that will further lead to stoichiometric aluminum oxide. Furthermore, a study on the binding of O_2 onto transition metals revealed high sensitivity of the overlap populations obtained in what concerns the type of basis set used.[48] Employing a triple-ζ all electron basis set avoids orbital overlap artifacts due to the rigidity of the ECP approach for describing the charge-exchange reactions involving a small atom such as Al. Additionally, the limitations of the double- ζ basis sets for describing the perturbed orbitals of Al when these interact with O are avoided.[49] An all electron basis set was used for all the calculations involving the clusters of the Al_{50} type. It is known that the cohesive energy of Al clusters with sizes ranging from 36 to 72 Al atoms shows only small fluctuations with cluster

size.[50] For the first ionization energy of closed shell Al clusters, convergence within less than 0.25 eV occurs already for clusters larger than 30 Al atoms.[51] Furthermore, the PBE0 density functional has demonstrated very good accuracy for describing electronic and structural properties of Al_9 type of clusters.[29] Additionally, the due to bonding with the O atoms of O_2, the loss of electron density from the Al atoms of the Al_{50} cluster is delocalized over the whole cluster and implies a loss of ≈0.04 e^-/Al atom. Based on this, we employed the Al_{50} model for the investigations of O_2 adsorption mechanisms.

Oxygen on pure Al_{50} and $Al_{50}Al_{ad}$ clusters

The optimized structures of the clusters $Al_{50}Al_{ad}$ and Al_{50} are shown in Figures 1a and 1b respectively. All clusters used in this study are in the singlet spin state as this is the favored spin state previously found for Al clusters of this size.[52] In order to achieve this, when necessary, an H atom was bound to an Al atom situated in the opposite side of the (111) surface of the cluster, as shown in Figure 1b. The spatial coordinates of the H atom were allowed to relax during geometry optimizations.

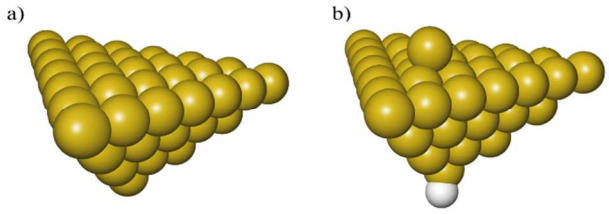

Figure 1. Clusters of 50 (a), (Al_{50}) and 51 (b) ($Al_{50}Al_{ad}$) Al atoms used to study the reactions of O_2. An H atom was added to the cluster $Al_{50}Al_{ad}$ in order to maintain the closed shell singlet spin state. Al (●), H (●).

The products of the reaction of O_2 with the clusters of Figure 1 are shown on Figure 2. For the molecular adsorption, the O_2 molecule shows a preference for a geometry almost parallel to the surface plane. This is in agreement with previous literature data.[17] For each product is also shown the plot of the respective overlap population densities of states (OPDOS) between the O atoms and the Al cluster (Figure 2). Also shown is the contribution of the orbitals of the O atoms to the electronic densities of states of the products. Positive OPDOS values correspond to bonding overlap while negative values correspond to anti-bonding overlap between the cluster and the oxygen atoms. It can be seen that the contribution of the O atoms orbitals for the newly formed electronic states is smaller than 50 % in all the cases. This indicates that the larger contribution for the new bonding states formed upon adsorption of O atoms come from the clusters populated electronic states. In turn this is an indication of delocalization of electronic density from the clusters to the O atoms in order to form the resulting bonding states, ultimately leading to the oxidation of the surface site where the O atoms adsorb. This is consistent with previous observations of bonding of radicals onto metal surfaces.[53] We recall that when the O-O bond in O_2 undergoes splitting—and before any electronic relaxation of the newly formed O atoms orbitals occurs—the O atoms are radical species with an open shell electronic structure. The interactions with the surface causes displacement of electron density from the surface in order to form the bonded states that will lead to a closed-shell electronic structure of the complex: adsorbate-adsorption site.[5] The extent of the interactions between the adsorbate O radicals and the surface will depend on how close in energy are the populated electronic states of the O radicals and those of the surface—in this case the cluster Fermi level. If the difference is large, the newly formed states are more diffuse in nature. If the difference is small the newly formed states are less diffuse in terms of their energies. This model is consistent with the OPDOS plots shown in Figure 2. For the case of the cluster with the surface adatom (Figure 2e)—which has

electronic states that lay closer to the O molecule than the case of the perfect (111) surface (Figure 2b)—upon molecular adsorption of O_2 the newly formed states are less diffuse in energy than for the case of the perfect surface. Additionally, for the surface with the adatom, also the contribution of the O orbitals to bonding is larger than for the case of the perfect surface. This indicates that the delocalization of electronic density from the surface to the O_2 molecule in order to form the molecular adsorption product is smaller for the case when the surface adatom is present when compared to the case of the perfect surface. Similarly, for the binding of O atoms, the contribution of these atoms orbitals to the resulting bonding states is larger for the case of the surface with an adatom when compared with the perfect surface. This means that for Al(111), when a surface adatom is present, the bonding between O atoms and the surface has more covalent character than for the case when the O atoms bind to the perfect (111) surface. This has implications on the molecular and dissociative adsorption energies of O_2. The molecular adsorption is 0.5 eV more exothermic when a surface adatom is present, $\Delta E_{ads,mo}$ (O_2–$Al_{50}Al_{ad}$) = -2.97 eV, when compared to the adsorption onto the perfect surface, $\Delta E_{ads,mo}$ (O_2–Al_{50}) = -2.47 eV. For dissociative adsorption of O_2, the difference in energy is smaller with the adsorption onto the surface with an adatom slightly less exothermic than the perfect surface: $\Delta E_{ads,dis}$ (O_2–$Al_{50}Al_{ad}$) = -8.53 eV; $\Delta E_{ads,dis}$ (O_2–Al_{50}) = -8.64 eV. The reason for this is that even though it is more favorable—from an electronic structure point of view, due to more similarities on their energy levels—to bind the O atoms onto the surface containing the adatom, for this case, the surface site where the O atoms bind to also goes through a more extensive reconstruction when compared to the case of the perfect surface. This has an energetic cost associated[54] and the energy initially gained due to the presence of the adatom is in this case decreased due to the energetic penalty involved in the reconstruction of the surface. This fact is not always verified for other dopants as it will be shown in the next section. The inclusion of the dispersion energy computed

with a term of the D3 type leads to slightly more exothermic adsorption energies: ≈0.11 eV for molecular adsorption and ≈0.16 eV for dissociative adsorption (Table 1) for both the clean surface and the surface with adatom respectively. An increase in the exothermicity of adsorption due to the inclusion of dispersion effects is expected and is in agreement with literature data.[41]

Table 1. Electronic adsorption energies for different modes of adsorption of O_2 onto the (111) surface of Al clusters. Al_{50} —flat (111) surface (Figure 1a); $Al_{50}Al_{ad}$ —(111) surface with a Al adatom (Figure 1b). ΔE_{mo} (molecular adsorption); ΔE_{dis} (dissociative adsorption). To the values labeled with – D3 has been added a D3 type dispersion correction component to the energy. All values in eV.

Cluster		O_2 adsorption			
		ΔE_{mo}	ΔE_{mo} – D3	ΔE_{dis}	ΔE_{dis} – D3
Al_{50}	Figure 1 a	-2.465	-2.580	-8.644	-8.800
$Al_{50}Al_{ad}$	Figure 1 b	-2.966	-3.084	-8.525	-8.689

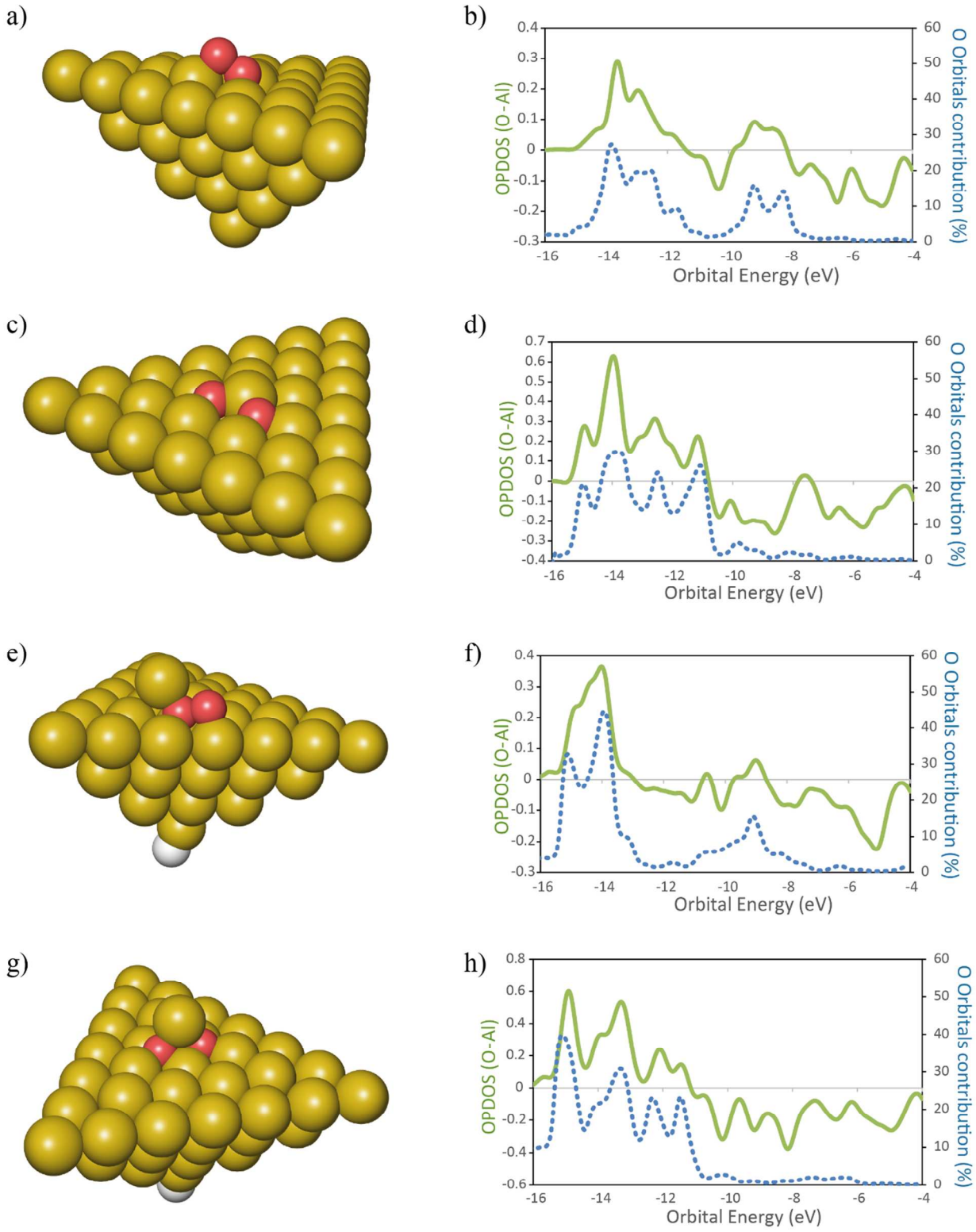

Figure 2. Products of adsorption of O_2 onto Al_{50} (figures a, c) and $Al_{50}Al_{ad}$ (figures e, g) clusters. In the plots are represented the overlap population densities of electronic states (OPDOS) (—)—

resultant from the overlap between the O atoms states and the cluster states—and the contribution of the O atoms orbitals to the final states (···) both as a function of orbital energy (eV). Only populated states are shown. a) and e) products of the molecular adsorption of O_2; c) and g) products of the dissociative adsorption of O_2. The corresponding adsorption energies are given in Table 1. Al (●), O (●) H (●). OPDOS > 0 = bonding interactions; OPDOS < 0 = anti-bonding interactions.

The effect of the presence of Si, Mg, Cu, Sc, Zr and Ti on the molecular and dissociative adsorption of O_2 onto Al(111).

In this section we report investigations on the effect of the presence of different atomic elements on the adsorption of O_2 onto Al(111). We also studied the geometric effects that accompany the placement of dopant atoms at the surface, by placing these atoms in two distinct geometries. The dopant atoms were placed both as an adatom and as a substituent for a surface Al atom, occupying an substitutional site at the Al(111) surface.

The geometries of the products of dissociative adsorption of O_2 and their corresponding OPDOS plots are shown in Figure 4 (dopants in adatom geometries) and Figure 5 (dopants in substitutional position geometries). The molecular adsorption products are shown in Figure 3. The corresponding adsorption energies are given in Table 2.

Table 2. Electronic energies for different modes of adsorption of O_2 onto the (111) surface of Al clusters. $Al_{49}X_{sub}$ –flat (111) surface with the dopant *X* in a substitutional surface position; $Al_{50}X_{ad}$ –(111) surface with a dopant in an adatom position. ΔE_{mo} (molecular adsorption); ΔE_{dis} (dissociative adsorption). To the values labeled with – D3 has been added a D3 type dispersion correction component to the energy. All values in eV. References in parentheses are the number of the respective figure showing the product structure; n/a means that the level of theory used could not predict the molecular adsorption product of O_2 for the respective cluster.

Dopant	**Geometry**	**O_2 adsorption**			
		ΔE_{mo}	ΔE_{mo} – D3	ΔE_{dis}	ΔE_{dis} – D3
Si	substitutional	-2.335 (3g)	-2.425 (3g)	-8.090 (5a)	-8.272 (5a)
	adatom	n/a	n/a	-8.299 (4a)	-8.463 (4a)
Mg	substitutional	n/a	n/a	-8.800 (5c)	-8.955 (5c)
	adatom	-3.377 (3a)	-3.494 (3a)	-8.006 (4c)	-8.172 (4c)
Cu	substitutional	n/a	n/a	-6.370 (5e)	-6.551 (5e)
	adatom	n/a	n/a	-8.163 (4e)	-8.332 (4e)
Sc	substitutional	n/a	n/a	-8.065 (5g)	-8.191 (5g)
	adatom	n/a	n/a	-9.206 (4g)	-9.208 (4g)
Zr	substitutional	n/a	n/a	-7.554 (5i)	-7.713 (5i)
	adatom	-3.750 (3c)	-3.818 (3c)	-8.416 (4i)	-8.525 (4i)
Ti	substitutional	n/a	n/a	-2.822 (5k)	-2.918 (5k)
	adatom	-3.731 (3e)	-3.755 (3e)	-8.403 (4k)	-8.376 (4k)

1

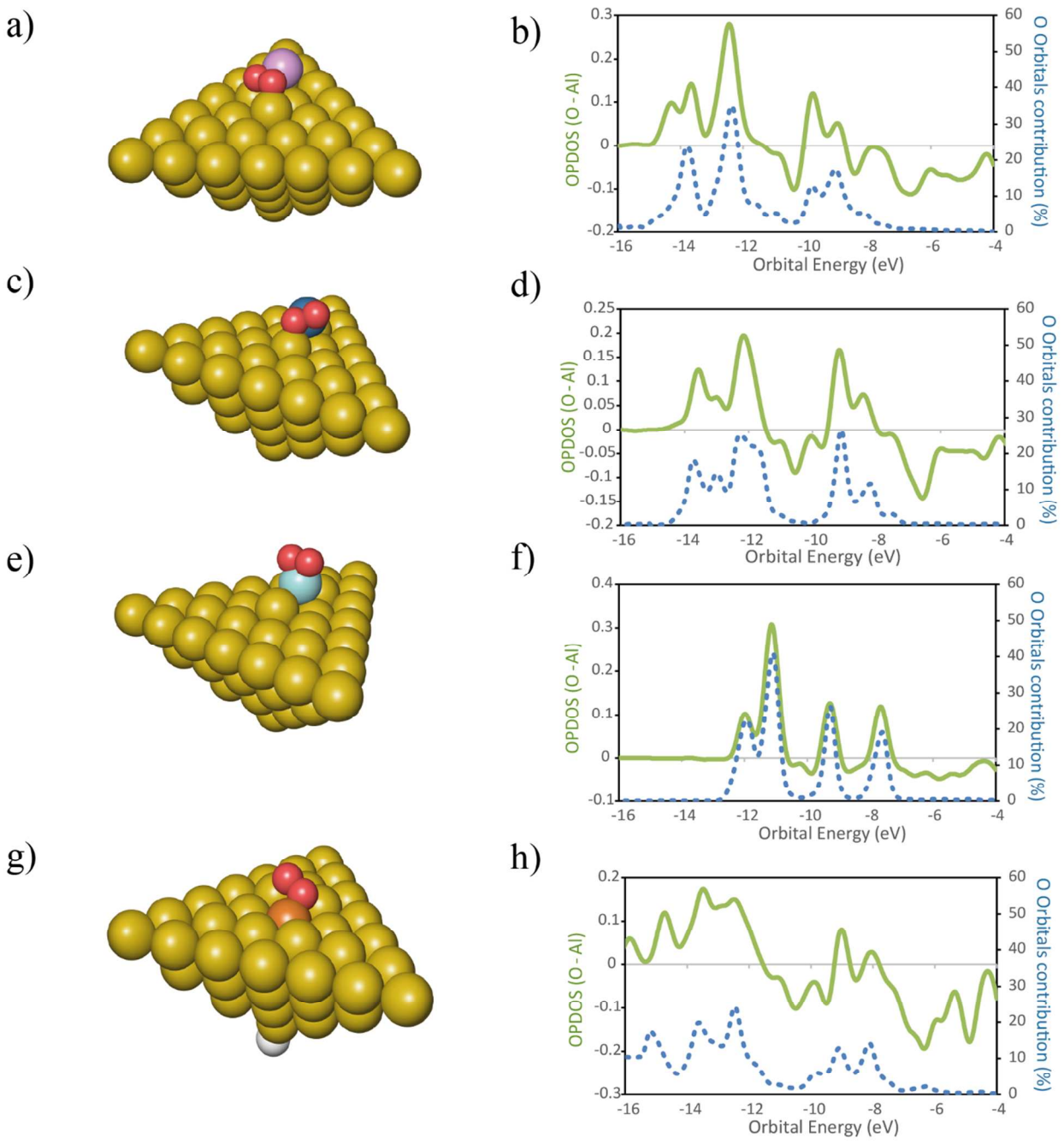

2

3 Figure 3. Structures of the products of molecular adsorption of O_2 onto clusters of the type
4 $Al_{50}X_{ad}$ (a,c,e) with *X* in adatom position: Mg (a) (●); Zr (c) (●); Ti (e) (●) and $Al_{49}X_{sub}$ (g) with
5 *X* placed as a surface substitutional atom: Si (g) (●). Al (●), H (●). In the respective plots are
6 represented the overlap population densities of electronic states (OPDOS) (—)—resultant from

the overlap between the O atoms states and the cluster states—and the contribution of the O atoms orbitals to the final states (···) both as a function of orbital energy (eV). Only populated states are shown. OPDOS > 0 = bonding interactions; OPDOS < 0 = anti-bonding interactions.

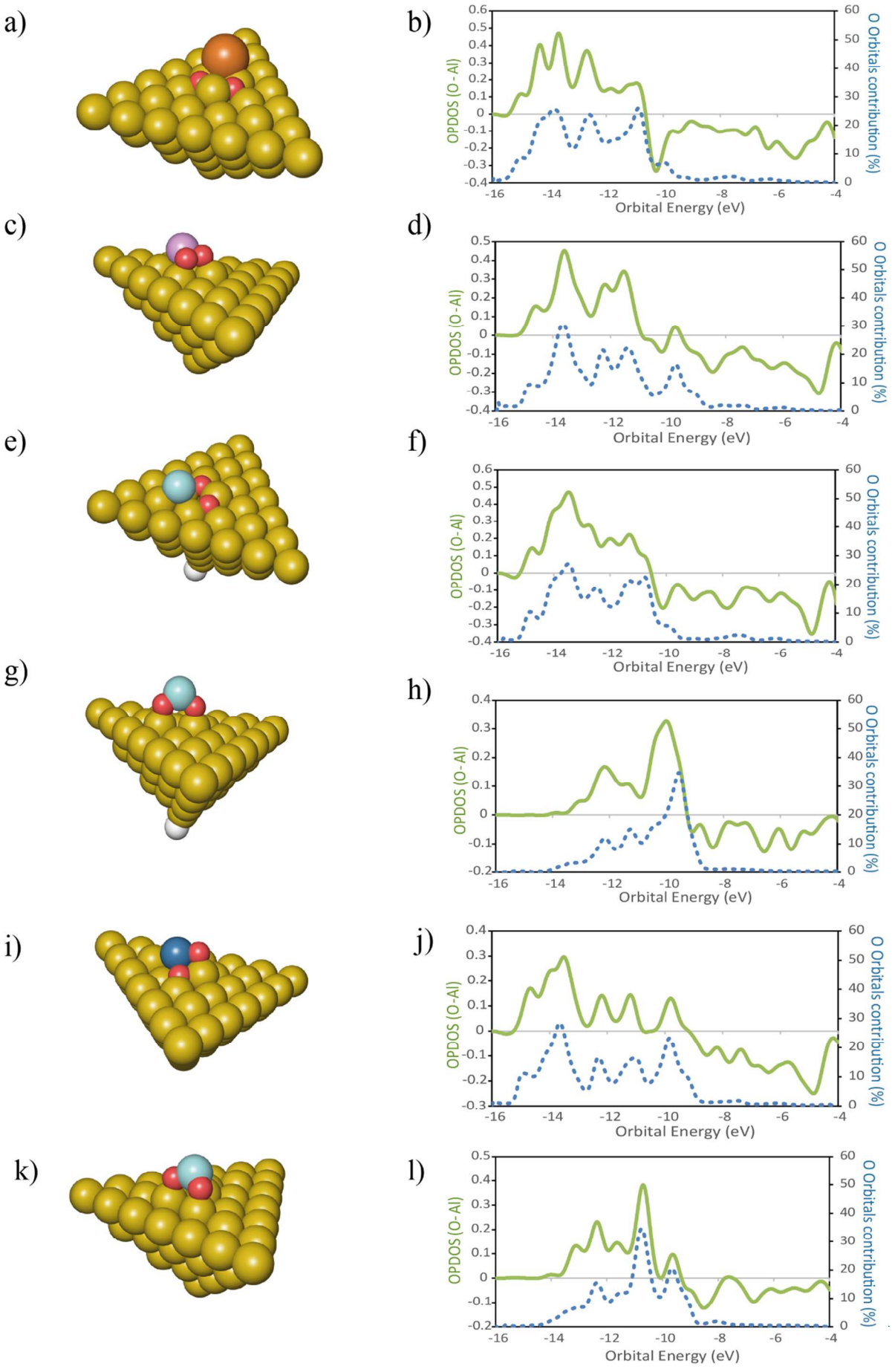
a)
b)
c)
d)
e)
f)
g)
h)
i)
j)
k)
l)
OPDOS (O - Al)
O Orbitals contribution (%)
Orbital Energy (eV)

Figure 4. Structures of the products of dissociative adsorption of O_2 onto clusters of the type $Al_{50}X_{ad}$. With *X* = Si (a,b) (●); Mg (c,d) (●); Cu (e,f) (●); Sc (g,h) (●); Zr (i,j) (●); Ti (k,l) (●). *X* placed as a surface adatom. Al (●), H (●). In the plots are represented the overlap population densities of electronic states (OPDOS) (—)—resultant from the overlap between the O atoms states and the cluster states—and the contribution of the O atoms orbitals to the final states (···) both as a function of orbital energy (eV). Only populated states are shown. OPDOS > 0 = bonding interactions; OPDOS < 0 = anti-bonding interactions

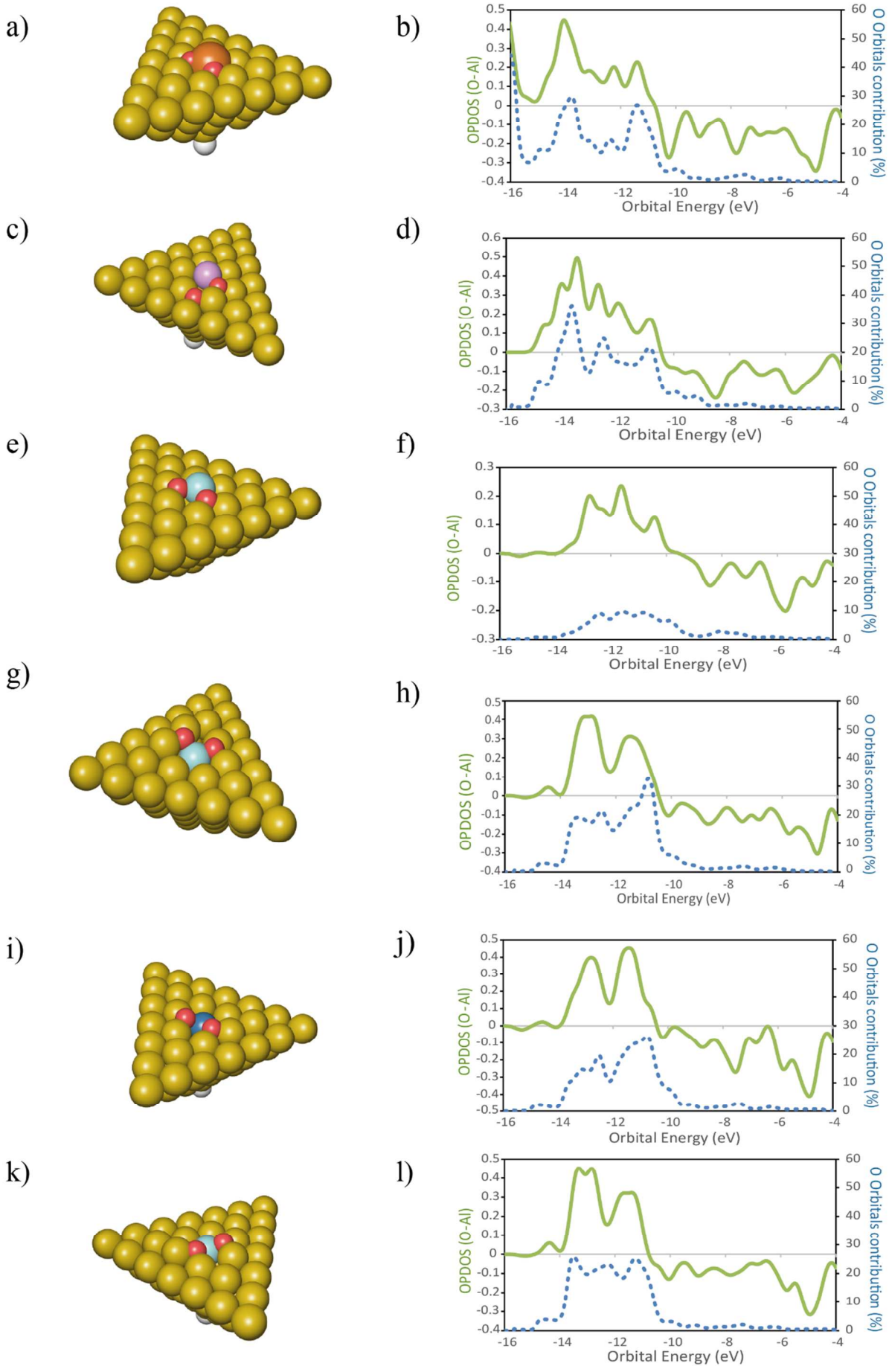
a)
b)
c)
d)
e)
f)
g)
h)
i)
j)
k)
l)
OPDOS (O-Al)
O Orbitals contribution (%)
Orbital Energy (eV)

Figure 5. Structures of the products of dissociative adsorption of O_2 onto clusters of the type $Al_{49}X_{sub}$. With X = Si (a,b) (●); Mg (c,d) (●); Cu (e,f) (●); Sc (g,h) (●); Zr (i,j) (●); Ti (k,l) (●). X placed as a surface substitutional adatom. Al (●), H (●). In the plots are represented the overlap population densities of electronic states (OPDOS) (—)—resultant from the overlap between the O atoms states and the cluster states—and the contribution of the O atoms orbitals to the final states (···) both as a function of orbital energy (eV). Only populated states are shown. OPDOS > 0 = bonding interactions; OPDOS < 0 = anti-bonding interactions

Only for some dopant atoms and geometries the level of theory here employed predicted molecular adsorption products of O_2. For the remaining cases, when placed at the surface, the O_2 molecule splits without an energy barrier. It has been suggested that when O_2 adsorption is computed with DFT, the spontaneous splitting of the molecule occurs whenever the computed LUMO of O_2 lays at energies more negatives than the computed HOMO (Fermi level) of the surface and in this way a spontaneous, barrierless charge transfer from the surface to the O_2 molecule would occur leading also to a barrierless splitting of O_2.[22] This fact was not confirmed with our calculations and no correlation exists between barrierless splitting of O_2 and the relation between the LUMO of this molecule and the HOMO of the surfaces. Upon charge transfer from the surface to the O_2 molecule, the rearrangement of the orbitals of the newly formed O_2^{n-} species will also be accompanied by a change in its bond length and such processes implicate an energy barrier.[13] The fact that DFT could not predict the existence of barriers for O_2 splitting in some cases is probably due to the fact that in those cases the energy barriers are small enough to lay within the error interval of computed energies for reactant structures.[55] Though, a detailed discussion of this topic is outside the scope of this work.

Molecular adsorption of O_2

The importance of the surface geometry effects in determining the mode of adsorption of O_2 is highlighted with the fact that for the adatom structures the elements that lead to a molecular adsorption product are Mg, Zr and Ti while for the substitutional structures only Si leads to a product of molecular adsorption of O_2. For the remaining cases, the O_2 molecule splits spontaneously when placed at the clusters surfaces. Even though we are not fully certain that this DFT description is correct—due to the lack of experimental data to support these findings— it is important to remark that the place occupied by the dopant atom at the surface has large implications in the mode of adsorption of O_2 and on the geometries of the products formed (Figure 5). This happens even for cases where the adsorption energies do not differ considerably (Table 2). Such similarity may lead to misinterpretations when concluding about adsorption modes of O_2 using only the adsorption energies to support those statements. As the surface geometric effects need to be considered we can only make fair comparisons of the electronic structure between the clusters where the dopant atom occupies the same geometry. For the case of the adatom geometries, the OPDOS plots reveal that for Mg, the contribution of the O atoms orbitals of O_2 for the states formed is less significant than for the cases of Zr and Ti. This observation is in agreement with the fact that both Zr and Ti have higher Pauling electronegativities of 1.33 and 1.54 respectively, when compared with that of Mg which is 1.31.[56] Because the molecular adsorption of O_2 occurs both via the interactions of its non-bonding electron pairs with the metal atoms and also due to the hybridization of the O_2 orbitals with the orbitals of the cluster,[57] a higher Pauling electronegativity of the metal atom means that these electrons involved in the bonding with O_2 are being more pulled away from the O_2 orbitals, become more delocalized and will occupy orbitals with less O_2 character than for the case where the electronegativity of the metal atom is smaller and does not exert a delocalization effect on the electrons of O_2 to such an extent. The value of $\Delta E_{ads,mo}$ (O_2–$Al_{50}X$) is less exothermic by

approximately 0.38 eV for the case of Mg than for the cases of Ti and Zr. These facts, together with the data from the OPDOS plots indicate that the molecular adsorption of O_2 is stronger for the cases where the newly formed states have more contribution from the orbitals of O_2 than for the cases where this contribution is smaller.

When the dopant atom occupies a substitutional position at the surface, the only case for which DFT predicted the existence of a molecular adsorption product was that of Si. Additionally, also for the non-doped Al surface, the adsorption of O_2 leads to a molecular adsorption geometry. This is a consequence of the similarities between the electronic structures of the two elements—Al and Si—as they occupy neighboring places in the same block in periodic table. Because the orbitals of the other elements investigated here differ more extensively from those of Al than the orbitals of Si, the energy barriers for splitting molecular adsorbed O_2 are possibly lower for surfaces doped with such elements.[58] It is plausible that the energy barriers are low enough to lay within the errors associated with the DFT calculations as described above.

Dissociative adsorption of O_2

For the cases where the dopant atoms occupy substitutional positions, the type of dopant has a very large effect on the dissociative adsorption energies of O_2. It can be seen in Table 2 that the least exothermic value is for the case of Ti doping while the dopant that leads to a more exothermic dissociation of O_2 is Mg. Even though the OPDOS plots for the Mg and Ti doped surfaces (Figures 4d and 4l respectively) do differ only moderately, the difference in exothermicity between these two extreme cases is 6 eV. This is because the dissociative adsorption of O_2 onto $Al_{49}Ti$ causes a more extensive adsorption site reconstruction than the equivalent process on $Al_{49}Mg$. The energy cost for displacing the surface atoms at the adsorption site is a factor that contributes to the decrease in the exothermicity of the adsorption process.[59] In the case of $Al_{49}Ti$, the bonding between the reconstructed adsorption site and the O atoms is not

exothermic enough to compensate for such energetic cost, causing the whole process of adsorption to be less exothermic. It can also be seen in Table 2 that the dissociative adsorption of O_2 on the surfaces where the dopant is an adatom is more exothermic than the corresponding process occurring on a surface where the dopant occupies a substitutional position. The only exception to this is for Si with a difference of 0.21 eV between both geometries. It can be seen in the OPDOS plots of both Si geometries that more anti-bonding states are populated for the case where Si occupies a substitutional position when compared to the adatom case. Overall, there are less differences in the OPDOS plots for the different dopants for the cases where the dopant atom is in a substitutional position.

For the adatom geometries, Sc and Ti are the cases that show larger differences in their OPDOS plots when compared with the remaining dopants (Figure 3). It can be seen on the product geometries (Figure 3) that for the cases of Sc and Ti, upon dissociative adsorption of O_2 these elements are displaced away from the surface, along the perpendicular direction, causing the dopant atoms to minimize their contact with the surface Al atoms. This makes the states of the resulting adsorption product that originate from these atoms states, to have more "free-atom-like" character and hence the less spread in energies in the OPDOS for these two cases when compared with the remaining dopants. For elements belonging to the third row of the periodic table, there are large differences in the resulting adsorption geometries and OPDOS—Cu different from the other third row two elements Sc and Ti. This can be attributed to the involvement of either *d* or *s* orbitals in the interactions with O atoms. Cu with the valence shell as $3d^{10}4s^{1}$ involves the more diffuse *s* orbitals in the bonding with O leading to an OPDOS which is more spread in energies—also the bonding with Al is stronger for this case because of the more symmetry favorable interactions between the Cu *s* and Al *p* orbitals. On the other hand, Sc with a valence shell $3d^{1}4s^{2}$ and Ti with $3d^{2}4s^{2}$, involve the more localized *d* orbitals in the bonding with O causing less

spread in the OPDOS and weaker interactions with Al, making the bonding between these elements and the Al surface easier to break due to the adsorption of O atoms. This effect can also be seen on the OPDOS plots of the substitutional dopant geometries. In this case, the transition metals that are located to the left of the periodic table—Sc, Ti and Zr—also lead to less spread in the energies of the bonding OPDOS than Cu when interacting with O atoms. For these dopants, it can be seen (Figure 4) that the bonding part of their OPDOS has two broad peaks close spaced and localized at around the same energies for the three cases, while the bonding OPDOS of Cu shows a more delocalized character.

The differences in adsorption energies between the adatom and substitutional atom geometries can be further analyzed in terms of the charge of the dopant atom. It has been previously observed that for neutral clusters of ($Al_{12}X$, with X = Mg, Al, Si), the dopant atom has a negative partial charge.[60] The authors found further that the magnitude of the dopant atom charge increases with the electronegativity and ionization potential (*IP*) of the dopant atom. In the cited work it was also found that for the same dopant atom, the charge is more negative for substitutionally placed dopants when compared to the case where the same dopant is an adatom. Translated to the results of this work, this implies that upon adsorption of O atoms, the more negatively charged the dopant atom is, the stronger it will bound to the O atoms because more charge is available to be displaced to the O atoms to form bonding states. Also, the polarization of the Al(111) surface will be less when the dopant atom ionization energies are closer to that of Al. This means that the higher the ionization energy of the dopant atom, the more the negative charge is located at this atom after forming bonded states with Al, and the more covalent character has the bonding between the dopant and Al. With basis on these observations, on the data of Table 2 and on what is stated above for the pure Al clusters, we found that for the same surface geometry, the higher is the ionization energy of the dopant atom, the more exothermic is

the adsorption of O atoms and the stronger are the bonds between the surface and the O atoms. This effect is visible in the plot of Figure 6. The plot shows the variation on the dissociative adsorption energy of O_2 as a function of the second ionization potential (IP_2) of the dopant atoms. The second ionization potential was chosen for the reasons that will be discussed in the next section. The O_2 adsorption data is for the dopants in substitutional position. The higher the IP_2 of the dopant atom, the more negatively charged is this atom and the stronger is the bonding with the O atoms. It can be seen that the dopant atoms that have a higher IP_2 lead to more exothermic dissociative adsorption of O_2. The correlation between both quantities supports the statement that the more covalent character has the bonding between the dopant atom and the Al surface, the stronger will be the bonds between the O atoms and the doped surface site.

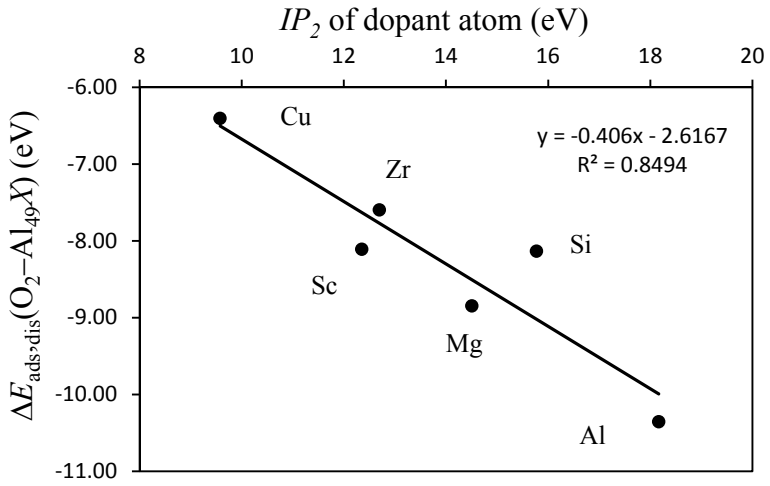

Figure 6. Plot of the dissociative adsorption energy of O_2 on an $Al_{49}X_{sub}$ cluster where X represents a surface dopant atom in a substitutional position ($\Delta E_{ads,dis}(O_2–Al_{49},X)$) (eV), as a function of the second ionization potential (IP_2) of the dopant atom (eV). X = Al, Si, Mg, Cu, Sc, Zr.

Mulliken electronegativity of the dopant atom and dissociative adsorption energy of O_2

The charge transfer between the dopant atom, *X*, and the Al(111) surface and further between the O atoms and the adsorption site (*X*Al(111)) can be analyzed based on Mulliken developments[61, 62] of the concepts of electronegativity (χ), ionization potential (*IP*), electron affinity (*EA*) and the significance of these quantities for describing charge transfer to and from atoms. For the present case the charge transfer and the surface polarizability at and in the near of the dopant site can be schematized as follows

$$X + \mathrm{Al(111)} \rightarrow X^{n+}\mathrm{Al(111)}^{n-} \quad \text{(R1)}$$

$$X^{n+}\mathrm{Al(111)}^{n-} + \mathrm{O_2} \rightarrow (\mathrm{OO})^{m-}X^{[(m/x)+]+(n+)}\mathrm{Al(111)}^{[(m/y)+]+(n-)} \quad \therefore (1/x + 1/y) = 1 \quad \text{(R2)}$$

where *n* and *m* can be either fractional or integer, and represent a partial or complete charge transfer respectively; R1 represents the reaction that leads to the placement of the initially charge neutral *X* atom at the surface; R2 represents the dissociative adsorption of O_2 that leads to the formation of the two surface adsorbed O atoms (OO). According to Mulliken definition of electronegativity, $\chi = [(IP+EA)/2]$.[61] For the different dopants, *X*, keeping the same substrate, Al(111), according to Mulliken original paper,[61] the amount of charge transferred from *X* to Al(111) in reaction R1 depends on the *first-stage electronegativity* (χ_1) of *X*. Consequently, in R2, for the series of different dopants, the difference in the amount of charge that is removed from the *X* (*m/x*) or from the Al surface (*m/y*) is dependent on the capability of the dopant to maintain the electrons on its orbitals when subject to a positive external potential such as that created by the O atoms. This property of the dopant atom now oxidized to the oxidation state *n*+ will depend on the *second-stage electronegativity* (χ_2) of the dopant. The property χ_2 has been defined by Mulliken as $\chi_2 = [(IP_2+EA_2)/4]$, where IP_2 is the second ionization potential of *X* (for forming the

species X^{2+}) and EA_2 is the double electron affinity. In the present case we used Mulliken formulation but employing the first electron affinity because reaction R1 also depends on this property of the dopant atom. We call this property the *modified second-stage electronegativity* (χ_{2m}). A plot of the dissociative adsorption energy of O_2 ($\Delta E_{ads,dis}(O_2{-}Al_{49}X)$) as a function of the *modified second-stage electronegativity* (χ_{2m}) of the dopant atom in substitutional position is shown in Figure 7. The good correlation seen between $\Delta E_{ads,dis}$ for O_2 and χ_{2m} demonstrates that the Mulliken concept is applicable to both the bonding between a dopant and a surface and also to the adsorption of O_2 to the doped surface site. It is important to note that this correlation is valid for the substitutional geometries of the adatoms. The geometric effects present when the dopant is in an adatom position cause a deviation from linearity when plotting the equivalent data. Also worth noticing is that the data for Al was included (doping with Al corresponds to the perfect Al surface) and corresponds to the ideal case where the surface where O_2 adsorbs onto, is non-polarized. This case is the case that leads to the more exothermic adsorption of O_2.

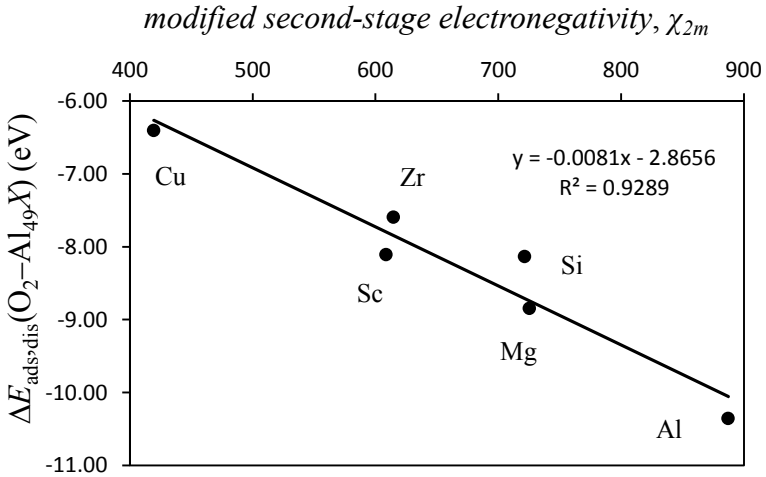

Figure 7. Plot of the dissociative adsorption energy of O_2 on an $Al_{49}X_{sub}$ cluster where X represents a surface dopant atom in a substitutional position ($\Delta E_{ads,dis}(O_2–Al_{49},X)$) (eV), as a function of the Mulliken *modified second-stage electronegativity*, χ_{2m} of the dopant atom. X = Al, Si, Mg, Cu, Sc, Zr.

The variation in adsorption energies for the geometries where the different dopants occupy an adatom position differs considerably from the variation found when the dopants occupy a substitutional position. For the different dopants in adatom geometries, the dissociative adsorption energies of O_2 vary only by 0.19 eV. The variation for the substitutional geometries is much larger: of 6.0 eV. This can be interpreted as a geometric effect that has implications on the mode of interaction between the orbitals of oxygen and those of the adsorption site. The adatom geometries lead to stronger bonding between the O atoms and the *X*Al(111) site because of the more adsorbate readily available spatial disposition of the orbitals of the dopant when this is an adatom. This is in contrast to the case when the dopant is substitutional at the surface. In the case of the adatom geometries, the interactions between O atoms and the adsorption site occur without extensive rearrangements of the surface—even though some displacement occurs for the dopant

atom in some cases, the energetic cost of this process is fairly low. In contrast, for the substitutional geometries, for the interactions between O atoms and the adsorption site to be maximized, some rearrangement of the adsorption site has to occur and this rearrangement decreases the exothermicity of the whole process of adsorption. Most importantly, for the substitutional geometries there are geometrical constrains for the orbitals of the O atoms to achieve the optimal interactions with the orbitals of the adsorption site when compared with the adatom geometries where these interactions are closer to the optimal case *i.e.* more free-atom-like character.

Conclusions

We investigated the effects of the presence of dopants on the Al(111) surface in the bonding with O_2 and O atoms and the modes of adsorption of these species. For the dissociative adsorption of O_2—adsorption of O atoms—different dopants at the surface lead to different types of bonding with the O atoms. This effect is dependent on both the type of dopant atom and the geometric placement of this atom at the surface. For dopants occupying a substitutional position at the Al(111) surface— *i.e.* replacing a surface Al atom—dopants with a higher ionization potential lead to a more covalent type of bonding with the Al surface. This situation causes a more exothermic adsorption of O_2 compared to when the bonding between the dopant and the Al surface is more ionic in nature. It is also demonstrated that the concepts of electronegativity as developed by Mulliken can be applied with success to predict the dissociative adsorption energy of O_2 onto Al(111) when the surface is doped with atoms that occupy substitutional positions. The larger the Mulliken electronegativity of the dopant atom, the stronger is the dissociative adsorption of O_2. This is because the more covalent is the bonding between the dopant and the Al surface the more negative charge is localized at the dopant atom. In turn, the more negative charge is available at the dopant atom the easier it is to delocalize this charge from the surface to

the O atoms. For the same underlying reasons, when the dopant atoms occupy an adatom geometry, the adsorption of O_2 is more exothermic when compared with the situation where the dopant is at the Al(111) surface in an substitutional position. For the same dopant atom, the adatom position allows for better overlap of electronic states between the surface adsorption site and the orbitals of O_2 leading to a stronger bonding when compared with the adsorption onto the surface with an adatom in substitutional position. Even though surface reconstruction leads to a better overlap between the electronic states of the O atoms and those of the surface, the energetic cost associated with this process is not always compensated by the formation of the new electronic states and in some cases, such as those involving the dopant Sc, reconstruction led to a less exothermic adsorption. Additionally, the PBE0 functional could not predict an energy barrier for O_2 dissociation for all the cases investigated here.

Acknowledgements

Financial support from the Swedish Foundation for Strategic Research (SSF, project ALUX) is gratefully acknowledged. The computations were performed on resources provided by the Swedish National Infrastructure for Computing (SNIC) at the National Supercomputer Center (NSC), Linköping.

References

1. I. P. Batra and L. Kleinman, *Journal of Electron Spectroscopy and Related Phenomena*, 1984, **33**, 175-241.

2. P. J. Eng, T. P. Trainor, G. E. Brown Jr., G. A. Waychunas, M. Newville, S. R. Sutton and M. L. Rivers, *Science*, 2000, **288**, 1029-1033.

3. G. E. Totten and D. S. MacKenzie, *Handbook of Aluminum volume 2 Alloy Production and Materials Manufacturing*, Marcel Dekker2003.

4. C. Carbogno, A. Groß, J. Meyer and K. Reuter, in *Dynamics of Gas-Surface Interactions*, eds. R. Díez Muiño and H. F. Busnengo, Springer Berlin Heidelberg2013, vol. 50, ch. 16, pp. 389-419.

5. J. Behler, K. Reuter and M. Scheffler, *Physical Review B*, 2008, **77**, 115421.

6. J. Trost, H. Brune, J. Wintterlin, R. J. Behm and G. Ertl, *The Journal of Chemical Physics*, 1998, **108**, 1740-1747.

7. H. Brune, J. Wintterlin, R. J. Behm and G. Ertl, *Physical Review Letters*, 1992, **68**, 624-626.

8. Y. Yourdshahyan, B. Razaznejad and B. I. Lundqvist, *Physical Review B*, 2002, **65**, 075416.

9. Y. F. Zhukovskii, P. W. M. Jacobs and M. Causá, *Journal of Physics and Chemistry of Solids*, 2003, **64**, 1317-1331.

10. A. Kiejna and B. I. Lundqvist, *Surface Science*, 2002, **504**, 1-10.

11. J. Jacobsen, B. Hammer, K. W. Jacobsen and J. K. No/rskov, *Physical Review B*, 1995, **52**, 14954-14962.

12. A. Kiejna and B. I. Lundqvist, *Surface Science*, 2002, **504**, 1-10.

13. F. Libisch, C. Huang, P. Liao, M. Pavone and E. A. Carter, *Physical Review Letters*, 2012, **109**, 198303.

14. J. Behler, B. Delley, S. Lorenz, K. Reuter and M. Scheffler, *Physical Review Letters*, 2005, **94**, 036104.

15. H.-R. Liu, H. Xiang and X. G. Gong, *The Journal of Chemical Physics*, 2011, **135**, 214702.
16. L. Österlund, I. Zoric-acute and B. Kasemo, *Physical Review B*, 1997, **55**, 15452-15455.
17. M. Kurahashi and Y. Yamauchi, *Physical Review Letters*, 2013, **110**, 246102.
18. C. Lacaze-Dufaure, C. Blanc, G. Mankowski and C. Mijoule, *Surface Science*, 2007, **601**, 1544-1553.
19. M. Schmid, G. Leonardelli, R. Tscheließnig, A. Biedermann and P. Varga, *Surface Science*, 2001, **478**, L355-L362.
20. F. Sebastian, E.-K. Lydia, V. E. Sergey, E. T. Oleg, S. Christoph, L. Peter, A. K. Konstantin, V. C. Evgueni, V. K. Tatyana, I. G. Vladimir, B. Hendrik, B. Matthias and R. Friedrich, *New Journal of Physics*, 2014, **16**, 075013.
21. G. Itziar, B. Juan, M. Jörg, J. I. Juaristi, A. Maite and R. Karsten, *New Journal of Physics*, 2012, **14**, 013050.
22. H.-R. Liu, H. Xiang and X. G. Gong, *The Journal of Chemical Physics*, 2011, **135**, -.
23. K. Honkala and K. Laasonen, *Physical Review Letters*, 2000, **84**, 705-708.
24. L. C. Ciacchi and M. C. Payne, *Physical Review Letters*, 2004, **92**, 176104.
25. P. Deák, *physica status solidi (b)*, 2000, **217(1)**, 9-21.
26. Jaguar, version 7.9, Schrödinger, LLC, New York, NY, 2012.
27. K. Burke, M. Ernzerhof and J. P. Perdew, *Chemical Physics Letters*, 1997, **265**, 115-120.
28. C. Adamo and V. Barone, *The Journal of Chemical Physics*, 1999, **110**, 6158-6170.
29. V. O. Kiohara, E. F. V. Carvalho, C. W. A. Paschoal, F. B. C. Machado and O. Roberto-Neto, *Chemical Physics Letters*, 2013, **568–569**, 42-48.
30. S. R. Miller, N. E. Schultz, D. G. Truhlar and D. G. Leopold, *The Journal of Chemical Physics*, 2009, **130**, 024304

31. P. J. Hay and W. R. Wadt, *The Journal of Chemical Physics*, 1985, **82**, 299-310.
32. S. Grimme, J. Antony, S. Ehrlich and H. Krieg, *The Journal of Chemical Physics*, 2010, **132**, 154104.
33. L. Goerigk and S. Grimme, *Physical Chemistry Chemical Physics*, 2011, **13**, 6670-6688.
34. X. Xu, H. Nakatsuji, M. Ehara, X. Lu, N. Q. Wang and Q. E. Zhang, *Chemical Physics Letters*, 1998, **292**, 282-288.
35. X. Lü, X. Xu, N. Wang, Q. Zhang, M. Ehara and H. Nakatsuji, *Chemical Physics Letters*, 1998, **291**, 445-452.
36. S. I. Gorelsky, Ottawa, ON, Revision 6.82 edn., 2013.
37. R. Hoffmann, *Solids and surfaces : a chemist's view of bonding in extended structures*, VCH Publishers, New York, NY, 1988.
38. T. Hughbanks and R. Hoffmann, *Journal of the American Chemical Society*, 1983, **105**, 3528-3537.
39. R. S. Mulliken, *The Journal of Chemical Physics*, 1955, **23**, 1833-1840.
40. M. N. D. S. Cordeiro, A. S. S. Pinto and J. A. N. F. Gomes, *Surface Science*, 2007, **601**, 2473-2485.
41. C. M. Lousada, A. J. Johansson, T. Brinck and M. Jonsson, *Physical Chemistry Chemical Physics*, 2013, **15**, 5539-5552.
42. F. Illas, N. López, J. M. Ricart, A. Clotet, J. C. Conesa and M. Fernández-García, *The Journal of Physical Chemistry B*, 1998, **102**, 8017-8023.
43. M. Fernández-García, J. C. Conesa, A. Clotet, J. M. Ricart, N. López and F. Illas, *The Journal of Physical Chemistry B*, 1998, **102**, 141-147.
44. S. González, C. Sousa and F. Illas, *Surface Science*, 2004, **548**, 209-219.
45. R. A. Evarestov, T. Bredow and K. Jug, *Physics of the Solid State*, 2001, **43**, 1774-1782.

46. F. Weigend and R. Ahlrichs, *Philosophical Transactions of the Royal Society A: Mathematical, Physical and Engineering Sciences*, 2010, **368**, 1245-1263.
47. J. E. Fowler and J. M. Ugalde, *Physical Review A*, 1998, **58**, 383-388.
48. M. Chen, S. P. Bates, R. A. van Santen and C. M. Friend, *The Journal of Physical Chemistry B*, 1997, **101**, 10051-10057.
49. M. Sierka, J. Döbler, J. Sauer, G. Santambrogio, M. Brümmer, L. Wöste, E. Janssens, G. Meijer and K. R. Asmis, *Angewandte Chemie International Edition*, 2007, **46**, 3372-3375.
50. A. K. Starace, C. M. Neal, B. Cao, M. F. Jarrold, A. Aguado and J. M. López, *The Journal of Chemical Physics*, 2008, **129**, 144702.
51. A. Aguado and J. M. López, *The Journal of Chemical Physics*, 2009, **130**, -.
52. R. Ahlrichs and S. D. Elliott, *Physical Chemistry Chemical Physics*, 1999, **1**, 13-21.
53. A. M. Pessoa, J. L. C. Fajín, J. R. B. Gomes and M. N. D. S. Cordeiro, *Surface Science*, 2012, **606**, 69-77.
54. D. P. Woodruff, in *Chemical Bonding at Surfaces and Interfaces*, ed. A. N. G. M. P. K. Nørskov, Elsevier, Amsterdam2008, pp. 1-56.
55. C. A. Farberow, J. A. Dumesic and M. Mavrikakis, *ACS Catalysis*, 2014, 3307-3319.
56. W. M. L. D. R. Haynes, *CRC handbook of chemistry and physics : a ready-reference book of chemical and physical data*, CRC Press, Boca Raton, Fla., 2011.
57. B. Yoon, H. Häkkinen and U. Landman, *The Journal of Physical Chemistry A*, 2003, **107**, 4066-4071.
58. W. V. Glassey and R. Hoffmann, *Surface Science*, 2001, **475**, 47-60.
59. S. Maier, P. Cabrera-Sanfelix, I. Stass, D. Sánchez-Portal, A. Arnau and M. Salmeron, *Physical Review B*, 2010, **82**, 075421.

60. A. Varano, D. J. Henry and I. Yarovsky, *The Journal of Physical Chemistry A*, 2010, **114**, 3602-3608.

61. R. S. Mulliken, *The Journal of Chemical Physics*, 1934, **2**, 782-793.

62. R. S. Mulliken, *The Journal of Chemical Physics*, 1935, **3**, 573-585.